Automatic Parameter Tuning for Plug-and-Play Algorithms Using Generalized Cross Validation and Stein's Unbiased Risk Estimation for Linear Inverse Problems in Computational Imaging

Canberk Ekmekci 1, Mujdat Cetin 1,2

Abstract

We propose two automatic parameter tuning methods for Plug-and-Play (PnP) algorithms that use CNN denoisers. We focus on linear inverse problems and propose an iterative algorithm to calculate generalized cross-validation (GCV) and Stein's unbiased risk estimator (SURE) functions for a half-quadratic splitting-based PnP (PnP-HQS) algorithm that uses a state-ofthe-art CNN denoiser. The proposed methods leverage forward mode automatic differentiation to calculate the GCV and SURE functions and tune the parameters of a PnP-HQS algorithm automatically by minimizing the GCV and SURE functions using grid search. Because linear inverse problems appear frequently in computational imaging, the proposed methods can be applied in various domains. Furthermore, because the proposed methods rely on GCV and SURE functions, they do not require access to the ground truth image and do not require collecting an additional training dataset, which is highly desirable for imaging applications for which acquiring data is costly and time-consuming. We evaluate the performance of the proposed methods on deblurring and MRI experiments and show that the GCV-based proposed method achieves comparable performance to that of the oracle tuning method that adjusts the parameters by maximizing the structural similarity index between the ground truth image and the output of the PnP algorithm. We also show that the SURE-based proposed method often leads to worse performance compared to the GCV-based proposed method.

Introduction

Various computational imaging problems, such as magnetic resonance imaging (MRI) [1], computational microscopy [2], radar imaging [3], and ultrasound imaging [4], can be described with an observation model for which the underlying image is observed through a linear forward operator representing the transformation applied by the imaging system followed by additive white Gaussian noise. For such observation models, the linear inverse problem refers to recovering the underlying latent signal from the observations, which is often ill-posed.

Plug-and-Play priors [5] is a framework that aims to solve imaging inverse problems by utilizing off-the-shelf denoisers as priors in model-based image reconstruction frameworks. Compared to end-to-end deep learning-based image reconstruction methods, such as deep unrolling methods [6], the main advan-

tage of the PnP priors is that it is more modular in the sense that after training a CNN denoiser, the same denoiser can be used as a prior for different configurations of the imaging setup. Because of its modularity and state-of-the-art performance, several studies [7, 8, 9, 10, 11] have developed variants of the original PnP algorithm based on the principles of PnP priors. Numerous works [12, 13, 14, 15] have applied the PnP algorithms to various computational imaging problems, and several works [13, 16, 17] have investigated the theoretical properties of PnP algorithms. For more details about the current status of the PnP literature, please refer to [18] and the references therein.

Although PnP algorithms have achieved state-of-the-art reconstruction performance for various imaging problems, careful tuning of the parameters of a PnP algorithm is needed to achieve such performance (see Figure 2 for an example). Even before the PnP priors and deep learning-based image reconstruction methods, a diverse set of methods, such as discrepancy principle [19], L-curve [20], generalized cross validation (GCV) [21], and Stein's unbiased risk estimation (SURE) [22], have been utilized to tune the parameters of image reconstruction methods. Motivated by this prior work, in this article, we propose GCV and SURE-based parameter tuning methods for a half-quadratic splitting-based (HQS-based) [25] PnP algorithm that uses a stateof-the-art Gaussian CNN denoiser called DRUNet [23]. To calculate the GCV and SURE functions for the PnP algorithm, we propose a computationally efficient algorithm that leverages forward mode automatic differentiation. We leverage the well-known parameter tying strategy employed by some of the PnP algorithms [5, 16] to reduce the number of parameters that need to be tuned and minimize the GCV and SURE functions using a grid search. The proposed methods do not require the knowledge of the underlying ground truth image and do not require collecting an additional dataset containing ground truth images and measurements. To evaluate the performance of the GCV and SURE-based tuning methods, we test those methods on deblurring and MRI experiments. We show that the GCV-based tuning method achieves comparable reconstruction performance to the oracle tuning method that uses the ground truth image to tune the parameters and that SURE-based tuning method often leads to over-regularization and worse performance in terms of reconstruction quality compared to the GCV-based tuning method.

We note that various semi-automatic parameter tuning strategies for PnP algorithms [16, 32, 33, 34, 23] have been proposed in the literature. As the main difference from those methods, the proposed methods tune all of the parameters automatically. Re-

¹ Department of Electrical and Computer Engineering, University of Rochester, Rochester, NY, USA.

² Goergen Institute for Data Science, University of Rochester, Rochester, NY, USA.

This work was partially supported by the National Science Foundation (NSF) under Grant CCF-1934962.

cently, Wei et al. [35] have proposed an automatic parameter tuning strategy using deep reinforcement learning. Compared to the proposed methods, the method proposed in [35] is more flexible in the sense that parameters of different iterations are not tied together, and it is applicable to non-linear inverse problems as well. Moreover, the inference time of the method in [35] is shorter than the methods proposed in this article. However, the method proposed in [35] requires an additional policy learning stage after training a CNN denoiser, introducing another set of hyperparameters that need to be tuned in the policy learning stage. Furthermore, although the method in [35] can handle different configurations of the same imaging problem, the policy learning stage must be repeated for different imaging problems. The proposed methods, on the other hand, do not require an additional training stage after training a CNN denoiser and can be used for different imaging problems straightforwardly without following an additional training stage, making the proposed methods more modular for different computational imaging problems.

Plug-and-Play Priors with HQS

Imaging process of several imaging modalities [1, 2, 3, 4] can be expressed by the following equation:

$$\mathbf{y} = \mathbf{A}\mathbf{x} + \mathbf{n},\tag{1}$$

where $\mathbf{y} \in \mathbb{F}^M$ is the vector containing the measurements; $\mathbf{A} \in \mathbb{F}^{M \times N}$ is the forward operator representing the transformation applied by the imaging system; $\mathbf{x} \in \mathbb{F}^N$ is the underlying image; and $\mathbf{n} \sim \mathscr{N}(\mathbf{0}, \sigma^2 \mathbf{I})$ is \mathbb{F}^M -valued additive white Gaussian noise, where \mathbb{F} stands for either \mathbb{R} or \mathbb{C} . In this work, we consider the general case for which $\mathbb{F} = \mathbb{C}$.

The main goal of an image reconstruction method is to recover the underlying image from the measurements, which is often referred to as the inverse problem. One way to solve the inverse problem is to formulate it as a regularized optimization problem defined by

$$\hat{\mathbf{x}} = \underset{\mathbf{x} \in \mathbb{C}^N}{\operatorname{argmin}} \left\{ \frac{1}{2} \|\mathbf{A}\mathbf{x} - \mathbf{y}\|_2^2 + \lambda \psi(\mathbf{x}) \right\}, \tag{2}$$

where $\lambda > 0$ is the regularization parameter, and $\psi : \mathbb{C}^N \to \mathbb{R}$ is the regularizer representing the prior knowledge about the underlying image. After choosing a suitable regularizer, such as total variation semi-norm [24], model-based image reconstruction methods solve the optimization problem in (2) using an appropriate splitting method such as HQS. After using the HQS method and replacing the prior dependent update step with a denoiser as proposed by the PnP idea, we obtain the following iterative reconstruction algorithm, which we refer to as the PnP-HQS algorithm.

$$\mathbf{z}^{(k)} = \mathbf{Q}^{(k)} (\mathbf{A}^{\mathsf{H}} \mathbf{y} + \boldsymbol{\mu}^{(k)} \mathbf{x}^{(k-1)})$$

$$\mathbf{x}^{(k)} = C_{\tau^{(k)}} (\mathbf{z}^{(k)}),$$
(3)

where $\mu^{(k)}$ is the penalty parameter at the k^{th} iteration; $\mathbf{Q}^{(k)} \triangleq (\mathbf{A}^{\text{H}}\mathbf{A} + \mu^{(k)}\mathbf{I})^{-1}$; the operator $C_{\tau^{(k)}}: \mathbb{C}^N \to \mathbb{C}^N$ is a complex Gaussian denoiser; and $\tau^{(k)}$ is the parameter controlling the strength level of the denoiser. Because most CNN denoisers are designed to handle real-valued inputs, we further assume that the complex Gaussian denoiser $C_{\tau^{(k)}}$ is defined by

$$C_{\tau^{(k)}}(\mathbf{z}) = D_{\tau^{(k)}}(\mathbf{z}_{\mathbf{R}}) + iD_{\tau^{(k)}}(\mathbf{z}_{\mathbf{I}}), \tag{4}$$

for all $\mathbf{z} \in \mathbb{C}^N$, where $D_{\tau^{(k)}}: \mathbb{R}^N \to \mathbb{R}^N$ is a real CNN Gaussian denoiser; i is the unit imaginary number; $\tau^{(k)}$ is the parameter controlling the strength level of the denoiser $D_{\tau^{(k)}}$; and the vectors $\mathbf{z}_{\mathbf{R}}, \mathbf{z}_{\mathbf{I}} \in \mathbb{R}^N$ are the real and imaginary parts of the complex vector \mathbf{z} , respectively.

Proposed Method

In this section, we present a computationally efficient algorithm to compute the GCV and SURE functions for the PnP-HQS algorithm and a grid search-based minimization procedure to minimize the GCV and SURE functions by using a parameter tying strategy.

Calculating the GCV and SURE for PnP-HQS

Suppose that the number of iterations of the PnP-HQS algorithm is fixed to $K \in \mathbb{Z}^+$. Then, we can interpret the output of the PnP-HQS algorithm $\mathbf{x}^{(K)}$ as a function of the measurement vector \mathbf{y} parameterized by the set $\theta \triangleq \{K, \mu^{(1)}, \cdots, \mu^{(K)}, \tau^{(1)}, \cdots, \tau^{(K)}\}$ containing all parameters of the PnP-HQS algorithm. Thus, we can write down the corresponding GCV function as follows [26].

$$GCV(\theta) = \frac{(1/M)\|\mathbf{y} - \mathbf{A}\mathbf{x}^{(K)}\|_{2}^{2}}{\left(1 - (1/M)\Re\left\{Tr\left\{\mathbf{A}\mathbf{J}(\mathbf{x}^{(K)}, \mathbf{y})\right\}\right\}\right)^{2}},$$
 (5)

where $\mathcal{R}\{\cdot\}$ computes the real part of a complex number, and $\mathbf{J}(\mathbf{x}^{(K)}, \mathbf{y})$ denotes the Jacobian of the output of the PnP-HQS algorithm evaluated at the measurement vector \mathbf{y} . Similarly, SURE function for the PnP-HQS algorithm is defined by [26]

SURE(
$$\theta$$
) = $\frac{1}{M} \|\mathbf{y} - \mathbf{A}\mathbf{x}^{(K)}\|_2^2 + \frac{2\sigma^2}{M} \mathcal{R}\{\text{Tr}\{\mathbf{A}\mathbf{J}(\mathbf{x}^{(K)}, \mathbf{y})\}\}, (6)$

where we have ignored the constant term that does not depend on θ . For the PnP-HQS algorithm, computational challenges in calculating the GCV and SURE functions are (i) calculating the trace of a high-dimensional matrix and (ii) calculating the Jacobian matrix $\mathbf{J}(\mathbf{x}^{(K)}, \mathbf{y})$ of the PnP-HQS algorithm.

To provide a computationally efficient trace estimate of a high dimensional matrix, several studies [27, 28] have provided a simple trace estimation method based on a lemma similar to the one provided below.

Lemma 1. Let $\mathbf{B} \in \mathbb{C}^{M \times M}$ be a matrix and \mathbf{b} be a \mathbb{R}^M -valued random vector with mean $\mathbf{0}$ and covariance matrix \mathbf{I} . Then,

$$Tr\{\mathbf{B}\} = \mathbb{E}[\mathbf{b}^{\top}\mathbf{B}\mathbf{b}],\tag{7}$$

where \mathbb{E} denotes the expectation operator.

Proof. Proof of this lemma directly follows from the properties of the trace and expectation operators. \Box

Using this lemma, we approximate the trace term of the GCV and SURE functions using a single realization of a standard multivariate normal random variable, which satisfies the conditions in Lemma 1. The resulting trace approximation has the following form:

$$\operatorname{Tr}\left\{\mathbf{A}\mathbf{J}(\mathbf{x}^{(K)},\mathbf{y})\right\} \approx \tilde{\mathbf{b}}^{\top}\mathbf{A}\mathbf{J}(\mathbf{x}^{(K)},\mathbf{y})\tilde{\mathbf{b}}$$
 (8)

where $\tilde{\mathbf{b}} \in \mathbb{R}^M$ is a realization of a standard multivariate normal random variable.

The remaining challenge is to compute the Jacobian matrix $J(\mathbf{x}^{(K)},\mathbf{y})$ of the PnP-HQS algorithm. We can obtain an iterative algorithm to calculate the Jacobian matrix $J(\mathbf{x}^{(K)},\mathbf{y})$ by manipulating the update equations of the PnP-HQS algorithm and using the chain rule, which is the result of the following lemma.

Lemma 2. For the PnP-HQS algorithm in (3), assume that $\mathbf{J}(\mathbf{x}^{(0)}, \mathbf{y})$ can be computed efficiently. Then, the Jacobian matrix $\mathbf{J}(\mathbf{x}^{(K)}, \mathbf{y})$ can be computed iteratively by following the update rule below

$$\mathbf{J}(\mathbf{x}^{(k)}, \mathbf{y}) = \mathbf{J}(C_{\tau^{(k)}}, \mathbf{z}^{(k)}) \mathbf{Q}^{(k)} (\mathbf{A}^H + \mu^{(k)} \mathbf{J}(\mathbf{x}^{(k-1)}, \mathbf{y})).$$
(9)

Proof. The PnP-HQS algorithm in (3) can be alternatively written as follows:

$$\mathbf{x}^{(k)} = C_{\tau^{(k)}} \left(\mathbf{Q}^{(k)} (\mathbf{A}^{\mathsf{H}} \mathbf{y} + \boldsymbol{\mu}^{(k)} \mathbf{x}^{(k-1)}) \right). \tag{10}$$

Then, the desired expression can be obtained by calculating Wirtinger derivatives of both sides and using the chain rule. \Box

We note that calculating the Jacobian matrix $\mathbf{J}(\mathbf{x}^{(K)},\mathbf{y})$ using this lemma assumes that $\mathbf{J}(\mathbf{x}^{(0)},\mathbf{y})$ is known. This is a reasonable assumption since this term often has an analytical form. For instance, if we choose $\mathbf{x}^{(0)} = \mathbf{A}^H \mathbf{y}$, then the Jacobian matrix $\mathbf{J}(\mathbf{x}^{(0)},\mathbf{y})$ is equal to \mathbf{A}^H .

Although we can compute the exact Jacobian matrix $J(\mathbf{x}^{(K)}, \mathbf{y})$ of the PnP-HQS algorithm by using Lemma 2, storing the Jacobian matrix in memory is computationally expensive for imaging problems. Since we only need the Jacobian-vector product $J(\mathbf{x}^{(K)}, \mathbf{y})\tilde{\mathbf{b}}$ to calculate the trace approximation in (8), we can multiply both sides of the update equation in (9) with $\tilde{\mathbf{b}}$ and end up with the following update rule.

$$\mathbf{j}(\mathbf{x}^{(k)}, \mathbf{y}) = \mathbf{J}(C_{\tau^{(k)}}, \mathbf{z}^{(k)}) \underbrace{\mathbf{Q}^{(k)}(\mathbf{A}^{\mathrm{H}}\tilde{\mathbf{b}} + \boldsymbol{\mu}^{(k)}\mathbf{j}(\mathbf{x}^{(k-1)}, \mathbf{y}))}_{\mathbf{r}^{(k)}} \quad (11)$$

where $\mathbf{j}(\mathbf{x}^{(k)}, \mathbf{y}) \triangleq \mathbf{J}(\mathbf{x}^{(k)}, \mathbf{y})\tilde{\mathbf{b}}$ is the vector that we store in memory. By using the definition of the complex denoiser $C_{\tau^{(k)}}$ in (4) and Wirtinger calculus, we can alternatively write the update rule in (11) as follows:

$$\mathbf{j}(\mathbf{x}^{(k)}, \mathbf{y}) = \frac{1}{2} \left[\mathbf{J}(D_{\tau^{(k)}}, \mathbf{z}_{R}^{(k)}) + \mathbf{J}(D_{\tau^{(k)}}, \mathbf{z}_{I}^{(k)}) \right] (\mathbf{r}_{R}^{(k)} + i\mathbf{r}_{I}^{(k)}). \tag{12}$$

We note that this update rule requires calculating four Jacobian-vector products at each iteration, where the Jacobian matrices are of the real CNN denoiser $D_{\tau^{(k)}}$ evaluated at either $\mathbf{z}_{R}^{(k)}$ or $\mathbf{z}_{I}^{(k)}$ and the vectors are either $\mathbf{r}_{R}^{(k)}$ or $\mathbf{r}_{I}^{(k)}$. In this work, we propose to use forward mode automatic differentiation (see [31] for a survey) to calculate those Jacobian-vector products. With forward mode automatic differentiation, those four Jacobian-vector products can be calculated exactly without storing and obtaining the Jacobian of the CNN denoiser explicitly as a matrix. Thus, we can evaluate the GCV and SURE functions efficiently for a given set θ of parameters by following the update rule in (12) together with forward mode automatic differentiation and the trace approximation in (8).

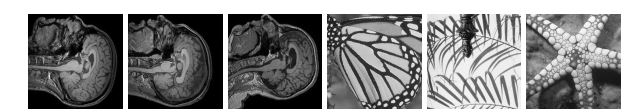


Figure 1. Test images used for the MRI and deblurring experiments. The image dimensions are 256×256 .

Minimization of GCV and SURE Functions

So far, we have provided a computationally efficient algorithm to evaluate the GCV and SURE functions for the PnP-HQS algorithm for a given set of parameters. The next step is to adjust the parameters of the PnP-HQS algorithm by minimizing the GCV or SURE functions. In this work, for simplicity, we consider a grid search to perform the minimization; however, a hybrid of a grid search and a derivative-free optimization method can be also used. We leave the investigation of such alternative optimization methods for future work.

At this point, we must note that performing a grid search is not computationally feasible since the number of elements of the set θ grows linearly with the number of iterations K. Fortunately, in the PnP literature, parameter tying strategies have been employed, e.g., [5, 16], to reduce the number of parameters of a PnP algorithm. By following [5, 16], we can introduce dependencies between the parameters as follows:

$$\tau^{(k)} = \sqrt{\lambda/\mu^{(k)}}$$
 and $\mu^{(k)} = \alpha\mu^{(k-1)}$, (13)

where $\lambda>0$ is a shared parameter between the denoiser strength and penalty parameters, and $\alpha>0$ is a scaling parameter controlling the increase of the penalty parameters. As a result, after parameter tying, the set θ containing the parameters of the PnP-HQS algorithm boils down to $\{K,\mu^{(0)},\alpha,\lambda\}$. The advantage of parameter tying is that the number of elements of the set containing the parameters of the PnP-HQS algorithm does not depend on K, making the grid search computationally feasible.

Experiments and Results

In this section, we evaluate the GCV and SURE-based parameter tuning methods on deblurring $(\mathbb{F}=\mathbb{R})$ and MRI experiments $(\mathbb{F}=\mathbb{C})$ and compare them with the oracle method (SSIM-optimal) that adjusts the parameters by maximizing the structural similarity index (SSIM) between the ground truth image and the output of the PnP-HQS algorithm. We first analyze the reconstruction performance of the proposed methods and provide both visual and quantitative results for different configurations of the deblurring and MRI setups. Then, we present experiments for which we tune only a subset of the four parameters using the proposed methods to investigate the stability of the parameter choices and to better visualize the closeness of the parameter choices to the oracle method in the SSIM sense.

Experimental Setup

For the deblurring experiments, we implemented the forward operator using a two-dimensional convolution operation with cyclic boundary conditions and used the blur kernels in [29]. For the MRI experiments, we used the subsampled Fourier transform to implement the forward operator. The test images used for the deblurring and MRI experiments are shown in Figure 1. The

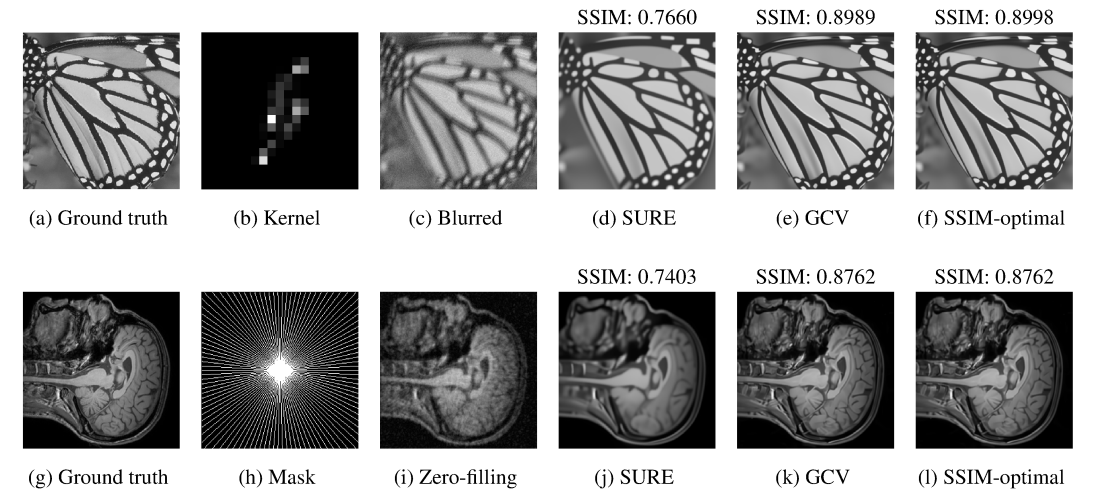


Figure 2. Visual reconstruction results for a deblurring test example and an MRI test example. For the deblurring example, the blur kernel is obtained from [29]. For the MRI example, the sampling mask has the radial pattern with the sampling rate of 20%.



Figure 3. Average SSIM results for the deblurring and MRI experiments. Blue color represents the results of the deblurring experiments, and green color represents the results of the MRI experiments. The eight blur kernels are obtained from [29].

MRI images are obtained from the IXI Dataset [30]. For the experiments, we normalized each test image so that each pixel has a value between 0 and 1, and unless otherwise stated, we fixed the noise level σ to 0.03.

For the deblurring and MRI experiments, we implemented the z-update step of the PnP-HQS algorithm using the Fourier transform. We used the DRUNet as a denoiser for the PnP-HQS algorithm and obtained its pre-trained weights from its public implementation in *https://github.com/cszn/DPIR/*. To ensure that the PnP-HQS algorithm is differentiable with respect to its input, which is required to have a well-defined Jacobian matrix for the PnP-HQS algorithm, we replaced each ReLU activation function of the DRUNet with the Softplus function whose beta value was set to 10^4 . To minimize the GCV and SURE functions, we performed a grid search with the parameters that were selected as follows. For the number of iterations K, we tried all of the integers in the interval [1,50]. For the stating point $\mu^{(0)}$ and the shared parameter λ , we tried 5 different values logarithmically spaced

between the interval $[10^{-5}, 10^{1}]$. For the scaling parameter α , we tried 5 values logarithmically spaced between the interval [1,2]. The implementation of the proposed methods is available online¹.

Visual Results

In this subsection, we visually evaluate the reconstruction performance of the proposed methods by comparing the resulting reconstructions to the reconstructions obtained by the oracle method. For different configurations of the deblurring and MRI setups, we tuned all four parameters of the PnP-HQS algorithm using the proposed methods. Visual results for a deblurring test example and an MRI test example are shown in Figure 2.

As can be seen in Figure 2, we observe that the GCV-based tuning method leads to reconstructions that are comparable to or the same as the reconstructions provided by the oracle tuning strategy. On the other hand, we observe that SURE-based tuning usually leads to over-regularization and results in the loss of fine details, such as thin edges and localized small structures, on the reconstructed image.

Quantitative Results

To quantitatively evaluate the reconstruction performance achieved by the proposed methods, we used the proposed methods to tune the parameters of the PnP-HQS algorithm for different configurations of the deblurring and MRI setups and calculated the SSIM index between the resulting reconstructions and the ground truth images. Figure 3 shows the resulting average SSIM results of the deblurring and MRI experiments, where the average SSIM values were calculated over the test images depicted in Figure 1.

As can be seen in Figure 3, the reconstruction quality of the PnP-HQS algorithm tuned by the GCV-based tuning method is comparable to the PnP-HQS algorithm tuned by the oracle method, which is consistent with our visual observations made in the previous subsection. On the other hand, we observe that the reconstruction performance achieved by the SURE-based tuning

¹https://github.com/cekmekci/SURE-GCV-PnP-Tuning

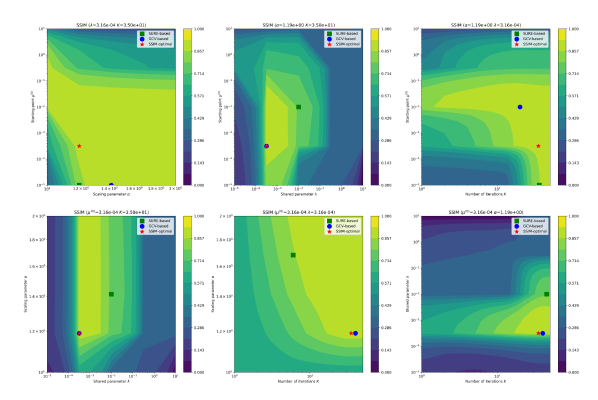


Figure 4. Parameter stability results for a deblurring test example. For each plot, we have tuned a pair of parameters while fixing the remaining two parameters to the oracle-optimal values and plotted the SSIM contour plot as a function of the tuned pair of parameters. Best viewed in zoom and color.

strategy is significantly inferior to the GCV-based tuning method and the oracle tuning strategy. This observation matches with our visual observations presented in the previous subsection, where we have observed that the SURE-based tuning often leads to overregularization.

Visualization of the SSIM Optimization Landscape

In the previous two subsections, we demonstrated the reconstruction performance achieved by the proposed methods visually and quantitatively. However, evaluating the stability of the parameter choices made by the proposed methods is challenging since it is not possible to visualize the parameter choices on a four-dimensional SSIM hypersurface. For this purpose, in this subsection, we fixed two of the parameters of the PnP-HQS algorithm to their SSIM-optimal values and adjusted the remaining two parameters using the proposed methods. We repeated this process for all pairs of the four parameters. Figure 4 and Figure 5 show the parameter choices made by the proposed methods and the oracle method and the contour plots of the SSIM surfaces for a deblurring test example and an MRI test example, respectively.

From Figure 4 and Figure 5, we observe that the GCVbased tuning methodology sometimes leads to different parameters than the SSIM-optimal parameters obtained by the oracle method, but achieves comparable reconstruction performance and similar SSIM values to the oracle method. Moreover, we observe that the GCV-based tuning strategy sometimes leads to the same parameters as the SSIM-optimal parameters obtained by the oracle method. On the other hand, we observe that the SUREbased tuning method often results in different parameters than the SSIM-optimal parameters and leads to worse reconstruction performance and suboptimal SSIM values compared to the GCVbased tuning method. These results show that the proposed parameter tuning methods are stable in the sense that the observations we made by tuning only a subset of the parameters match the observations made in the previous two subsections, where we tuned all of the four parameters.

Conclusion

In this paper, we have proposed an algorithm to calculate the GCV and SURE functions for the PnP-HQS computational

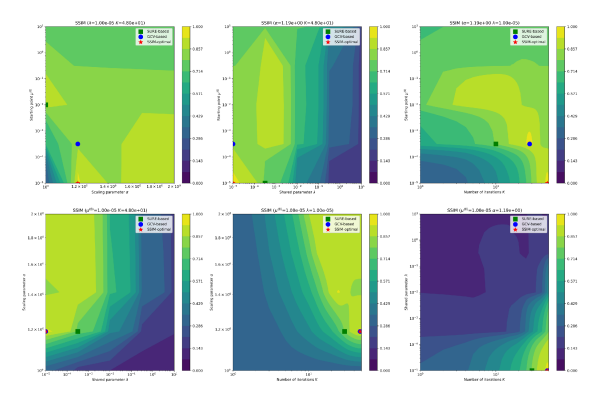


Figure 5. Parameter stability results for an MRI test example. For each plot, we have tuned a pair of parameters while fixing the remaining two parameters to the oracle-optimal values and plotted the SSIM contour plot as a function of the tuned pair of parameters. Best viewed in zoom and color.

imaging algorithm by using forward mode automatic differentiation. We have utilized parameter tying for the PnP-HQS algorithm to reduce the number of parameters that need to be tuned and to make the grid search used to minimize the GCV and SURE functions computationally feasible. The resulting parameter tuning strategies do not require access to the ground truth image and do not need an additional training dataset, which is desirable for practical computational imaging applications, especially for the ones for which collecting data is time-consuming and costly. In our experiments, we have evaluated the two strategies on deblurring and MRI and observed that the GCV-based tuning method can achieve comparable performance to the oracle method. On the other hand, we have observed that the SURE-based tuning strategy often leads to worse performance compared to the GCVbased tuning method. Our plans for future work are to apply the parameter tuning idea presented in this work to other variants of the PnP algorithms and to further investigate alternative optimization algorithms to minimize the GCV and SURE functions.

References

- J. A. Fessler, "Model-based image reconstruction for MRI," IEEE Signal Process. Mag., vol. 27, no. 4, pp. 81-89, Jul. 2010.
- [2] P. Sarder and A. Nehorai, "Deconvolution methods for 3-D fluorescence microscopy images," IEEE Signal Process. Mag., vol. 23, no. 3, pp. 32-45, May 2006.
- [3] L. C. Potter, E. Ertin, J. T. Parker, and M. Cetin, "Sparsity and compressed sensing in radar imaging," Proc. of IEEE, vol. 98, no. 6, pp. 1006-1020, Jun. 2010.
- [4] R. Lavarello, F. Kamalabadi and W. D. O'Brien, "A regularized inverse approach to ultrasonic pulse-echo imaging," IEEE Trans. on Med. Imag., vol. 25, no. 6, pp. 712-722, June 2006.
- [5] S. V. Venkatakrishnan, C. A. Bouman, and B. Wohlberg, "Plug-andplay priors for model based reconstruction," Proc. IEEE Glob. Conf. Signal Inf. Process., pp. 945-948, 2013.
- [6] V. Monga, Y. Li and Y. C. Eldar, "Algorithm unrolling: Interpretable, efficient deep learning for signal and image Processing," IEEE Signal Process. Mag., vol. 38, no. 2, pp. 18-44, March 2021.
- [7] K. Zhang, W. Zuo, S. Gu, and L. Zhang, "Learning deep CNN denoiser prior for image restoration," IEEE Conf. on Comp. Vis. and Pat. Recog., 2017.

- [8] T. Meinhardt, M. Moeller, C. Hazirbas, and D. Cremers, "Learning proximal operators: Using denoising networks for regularizing inverse imaging problems," IEEE Inter. Conf. on Comp. Vis., 2017.
- [9] U. S. Kamilov, H. Mansour, and B. Wohlberg, "A Plug-and-Play priors approach for solving nonlinear imaging inverse problems," IEEE Signal Process. Lett., vol. 24, no. 12, pp. 1872-1876, Dec. 2017.
- [10] Y. Sun, B. Wohlberg, and U. S. Kamilov, "An online Plug-and-Play algorithm for regularized image reconstruction," IEEE Trans. Comp. Imag., vol. 5, no. 3, pp. 395-408, Sep. 2019.
- [11] C. Ekmekci and M. Cetin, "What does your computational imaging algorithm not know?: A Plug-and-Play model quantifying model uncertainty", Proc. of the IEEE/CVF Inter. Conf. on Comp. Vis. (ICCV) Workshops, pp. 4018-4027, 2021.
- [12] A. Rond, R. Giryes, and M. Elad, "Poisson inverse problems by the Plug-and-Play scheme," Jour. of Vis. Comm. and Image Repres., vol. 41, pp. 96-108, 2016.
- [13] S. Sreehari et al., "Plug-and-Play priors for bright field electron tomography and sparse interpolation," IEEE Trans. on Comp. Imag., vol. 2, no. 4, pp. 408-423, Dec. 2016.
- [14] Y. Sun, S. Xu, Y. Li, L. Tian, B. Wohlberg, and U. S. Kamilov, "Regularized Fourier ptychography using an online Plug-and-Play algorithm," IEEE Inter. Conf. on Acous., Speech and Signal Process., pp. 7665-7669, 2019.
- [15] M. B. Alver, A. Saleem, and M. Cetin, "Plug-and-Play synthetic aperture radar image formation using deep priors," IEEE Trans. on Comp. Imag., vol. 7, pp. 43-57, 2021.
- [16] S. H. Chan, X. Wang, and O. A. Elgendy, "Plug-and-Play ADMM for image restoration: Fixed-point convergence and applications," IEEE Trans. on Comp. Imag., vol. 3, no. 1, pp. 84-98, March 2017.
- [17] E. K. Ryu, J. Liu, S. Wang, Xiaohan Chen, Z. Wang, and W. Yin, "Plug-and-Play methods provably converge with properly trained denoisers," Inter. Conf. on Machine Learning, 2019.
- [18] U. S. Kamilov, C. A. Bouman, G. T. Buzzard, and B. Wohlberg, "Plug-and-Play methods for integrating physical and learned models in computational imaging: Theory, algorithms, and applications," IEEE Signal Process. Mag., vol. 40, no. 1, pp. 85-97, Jan. 2023.
- [19] V. A. Morozov, "Methods for Solving Incorrectly Posed Problems", NY: Springer, pp. 32-64, 1984.
- [20] P. C. Hansen, "Analysis of Discrete Ill-Posed Problems by Means of the L-Curve," SIAM Review, vol. 34, no. 4, pp. 561-580, 1992.
- [21] P. Craven and G. Wahba, "Smoothing noisy data with spline functions," Numerische Mathematik, vol. 31, no. 4, pp. 377-403, 1979.
- [22] C. M. Stein, "Estimation of the mean of a multivariate normal distribution," Ann. Statist., vol. 9, no. 6, pp. 1135-1151, Nov. 1981.
- [23] K. Zhang, Y. Li, W. Zuo, L. Zhang, L. Van Gool, and R. Timo-fte, "Plug-and-Play image restoration with deep denoiser prior," IEEE Trans. on Patt. Anal. and Mach. Intell., vol. 44, no. 10, pp. 6360-6376, Oct. 2022.
- [24] A. Chambolle, "An algorithm for total variation minimization and applications," J. Math. Imag. Vis., vol. 20, no. 1, pp. 89-97, 2004.
- [25] D. Geman and C. Yang, "Nonlinear image recovery with half-quadratic regularization," IEEE Trans. on Image Process., vol. 4, no. 7, pp. 932-946, July 1995.
- [26] S. Ramani, Z. Liu, J. Rosen, J. -F. Nielsen, and J. A. Fessler, "Regularization parameter selection for nonlinear iterative image restoration and MRI reconstruction using GCV and SURE-based methods," IEEE Trans. on Image Process., vol. 21, no. 8, pp. 3659-3672, Aug. 2012.
- [27] M. F. Hutchinson, "A stochastic estimator of the trace of the in-

- fluence matrix for Laplacian smoothing splines," Comm. in Stat. Simul. and Comput., vol. 18, no. 3, pp. 1059-1076, 1989.
- [28] D. A. Girard, "A fast 'Monte-Carlo cross-validation' procedure for large least squares problems with noisy data", Numerische Mathematik, vol. 56, no. 1, pp. 1-23, 1989.
- [29] A. Levin, Y. Weiss, F. Durand, and W. T. Freeman, "Understanding and evaluating blind deconvolution algorithms," IEEE Conf. on Comp. Vis. and Patt. Recog., pp. 1964-1971, 2009.
- [30] D. Hill, S. Williams, D. Hawkes, and S. Smith, "IXI dataset: IXI information eXtraction from images project (EPSRC GR/S21533/02)" [Online]. Available: https://braindevelopment.org/ixi-dataset/
- [31] A. G. Baydin, B. A. Pearlmutter, A. A. Radul, and J. F. Siskind, "Automatic differentiation in machine learning: A survey," Jour. Mach. Learn. Res., vol. 18, no. 1, pp. 5595-5637, 2017.
- [32] K. Zhang, W. Zuo, S. Gu, and L. Zhang, "Learning deep CNN denoiser prior for image restoration," IEEE Conf. on Comp. Vis. and Patt. Recog., pp. 3929-3938, 2017.
- [33] T. Tirer and R. Giryes, "Image restoration by iterative denoising and backward projections," IEEE Trans. on Image Process., vol. 28, no. 3, pp. 1220-1234, March 2019.
- [34] X. Wang and S. H. Chan, "Parameter-free Plug-and-Play ADMM for image restoration," IEEE Inter. Conf. on Acous., Speech and Signal Process., pp. 1323-1327, 2017.
- [35] K. Wei, A. Aviles-Rivero, J. Liang, Y. Fu, H. Huang, and C.-B. Schonlieb, "TFPnP: Tuning-free Plug-and-Play proximal algorithms with applications to inverse imaging problems," Journ. of Mach. Lear. Res., vol. 23, no. 16, pp. 1-48, 2022.

Author Biography

Canberk Ekmekci is currently pursuing the Ph.D. degree at the University of Rochester, Rochester, NY, under the supervision of Prof. Mujdat Cetin. His research interests include machine learning, convex optimization, and linear inverse problems arising in computational imaging.

Mujdat Cetin is a Professor of Electrical and Computer Engineering and the Director of the Goergen Institute for Data Science at the University of Rochester. His research interests include computational imaging, bioimage analysis, and brain-computer/machine interfaces. Prof. Cetin is currently the Editor-in-Chief of the IEEE Transactions on Computational Imaging, a Senior Area Editor for the IEEE Transactions on Image Processing, as well as an Associate Editor for the SIAM Journal on Imaging Sciences and for Data Science in Science. He served as the Chair of the IEEE Computational Imaging Technical Committee and as the Technical Program Co-chair for five conferences. Prof. Cetin has received several awards including the IEEE Signal Processing Society Best Paper Award; the EURASIP/Elsevier Signal Processing Best Paper Award; the IET Radar, Sonar and Navigation Premium Award; and the Turkish Academy of Sciences Distinguished Young Scientist Award. He is a Fellow of IEEE.